

# *E* and *B* modes in the DPS in the context of STEP1

**Marco Hetterscheidt**

---

Patrick Simon, Thomas Erben, Hendrik Hildebrandt  
& Peter Schneider

IAEF, University of Bonn

STEP meeting, July 2005

## Deep Public Survey

Deep Public Survey (DPS) data has been taken by ESO Imaging Survey (EIS), reduced with the GaBoDS-pipeline.

Reduced & coadded data available, release paper in less than 1 month.

Pass-band	Exp. Time (s)	Lim. mag.	Area sq.deg.
U	61200	26.8	2.3
B	12600	26.0	2.0
V	9000	26.0	2.7
R	9000	26.3	3.3
I	27000	26.0	2.3

Limiting AB-mag:  $5\sigma$  in a  $2''$  aperture.

R-band: 222656 galaxies in the final weak lensing catalogue.

black: images taken with WFI@2.2m (8 CCDs, total area:  $34' \times 34'$ )

## GaBoDS-pipeline

Data is reduced with the GaBoDS-pipeline developed in Bonn; T. Erben et al. (AN 326, No. 6, 432-464, 2005).

The main scientific scope of the pipeline is to obtain images for weak lensing studies. It is almost fully automatic and can process all chips of a multi-chip camera in parallel.

For this a computer cluster with 38 nodes was purchased (Nodes: Athlon XP2800+ processor, 2 GB RAM, 300 GB; and a two processor master: Athlon XP2800+ processor, 4 GB RAM; altogether 45 TB hard disc space).

So we are well prepared for future large surveys (KIDS survey) which will be taken with OmegaCAM at the 2.6 m VLT Survey Telescope (VST) at Paranal.

OmegaCAM: 32 CCDs, total area:  $\approx 1 \text{ deg}^2$

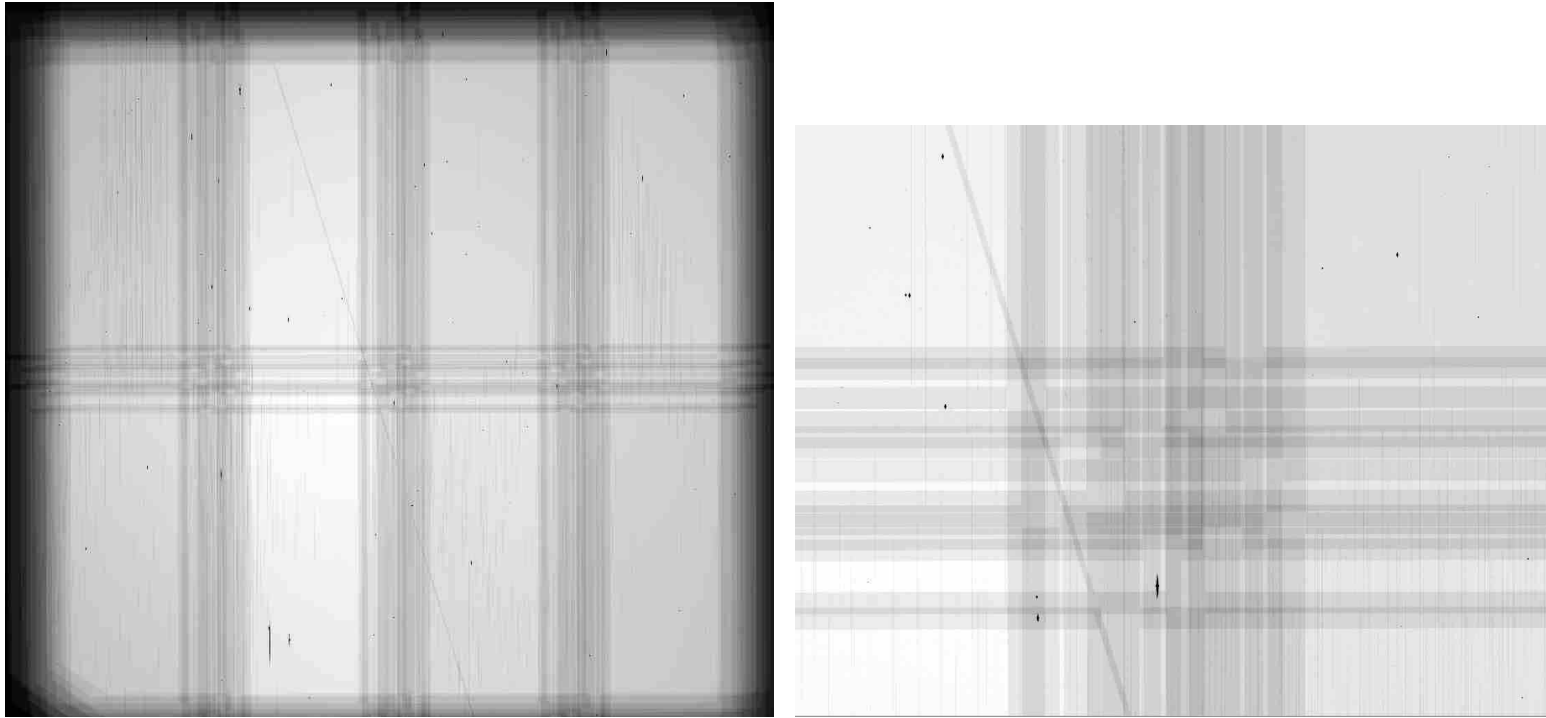
## Catalogue Creation

We utilise SExtractor to detect sources.

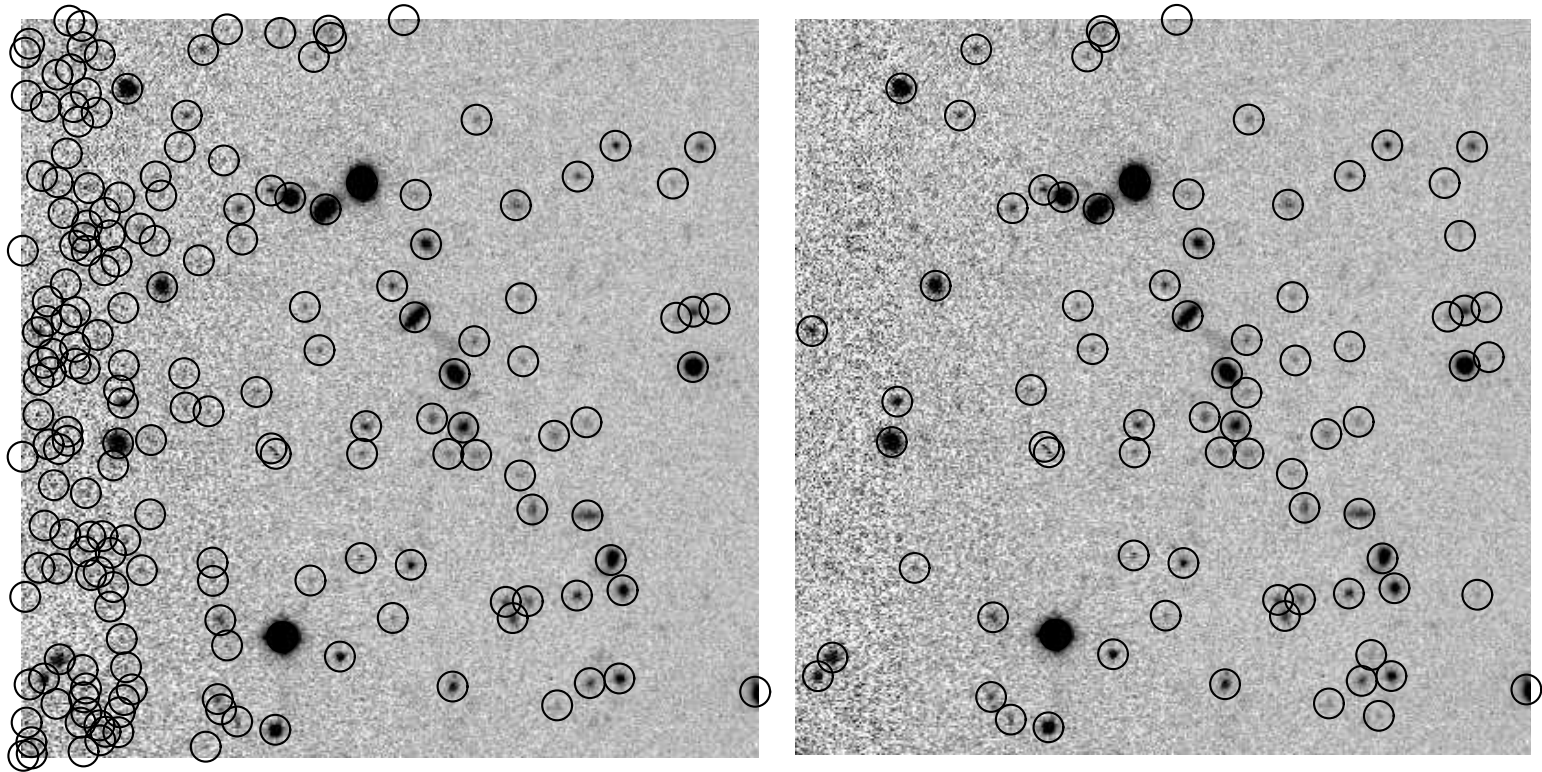
Weighting: For object detection we are using the weighting map of the reduction process.

The weighted image is smoothed with a Gaussian filter with a FWHM of 4 pixels.

The source extraction is done on the smoothed image, where we normally use 5 contiguous pixels with a flux  $1\sigma$  above the flux of the sky level noise.



The WEIGHT map is obtained by co-adding the normalised skyflats with all defects set to zero in the same way as the science images. It characterises the noise properties of a co-added science image. The lighter the colour, the higher the relative weight (the lower the noise) of the pixel. These maps are used by SExtractor for object detection.



SExtractor source catalogue obtained from the same mosaic (with an area of  $95'' \times 95''$ ) without (left) and with (right) a WEIGHT image as an additional SExtractor argument. The number of spurious detections in regions with higher noise is obvious when no WEIGHT image is used as an additional input.

## Our implementation of the KSB algorithm

3<sup>rd</sup> to 5<sup>th</sup> order 2D polynomial fit over the whole field to  $q(r_g^*)$  with 3  $\sigma$ -clipping.

Galaxy size  $r_g$  is SExtractor FLUX\_RADIUS.

Quadrupole estimate: interpolation,  $\theta_{\max} = 3r_g$  and  $\Delta\theta = 0.25$  pixel.

$P^\gamma$  correction:  $0.5 \text{tr}(P^\gamma)$ , no fit.

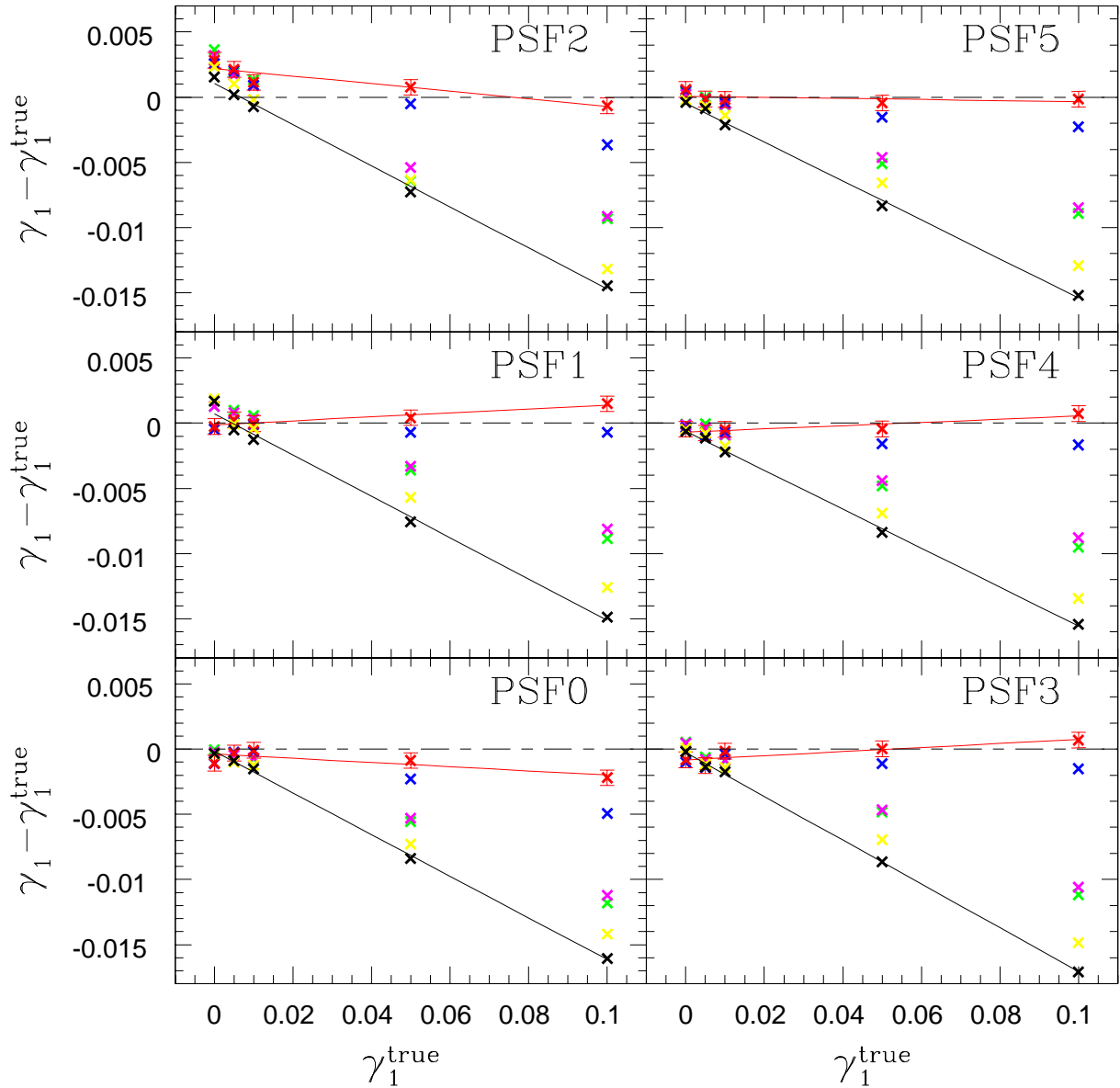
Cuts:  $P^\gamma > 0$  and  $|\gamma| < 0.8$ .

Weights:  $\langle \gamma^2 \rangle^{-1}$  of 20 neighbours in  $(r_g - mag)$ -plane.

NEW I:  $\gamma_{\text{corr}} = \gamma/0.88$  & size cut  $r_h > 1.1 r_h^*$

NEW II: full matrix calc., size cut  $r_h > 1.1 r_h^*$ ,  $|\gamma| < 1.4$

## STEP1: Shear estimates of $\gamma_1$

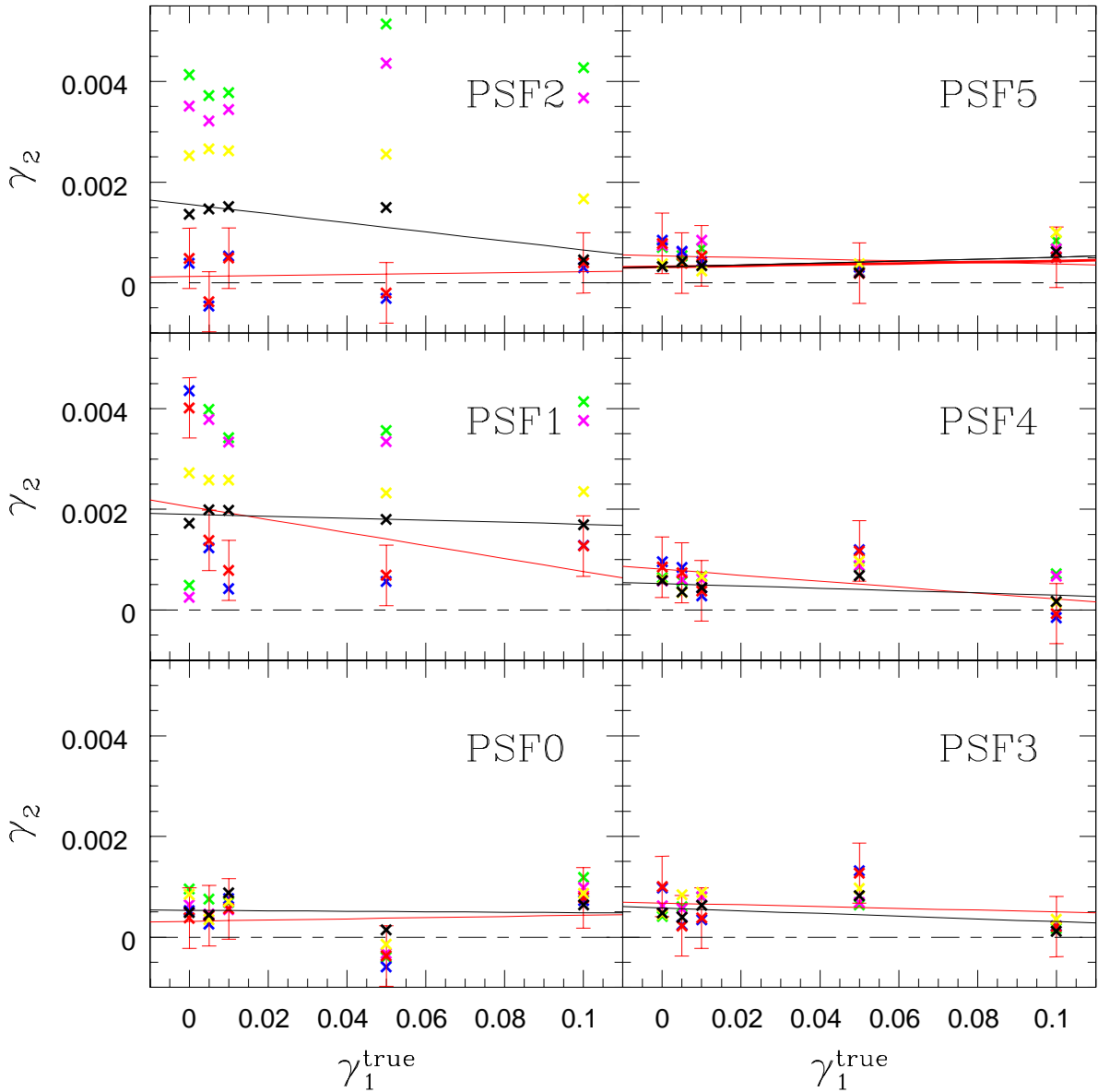


Black: old pipeline.

Red: after modifications: full matrix calculation,  $r_h > 1.1 r_h^*$ ,  $|\gamma| < 1.4$ , Hoekstra weight.



## STEP1: Shear estimates of $\gamma_2$



Black: old pipeline.

Red: after modifications: full matrix calculation,  $r_h > 1.1 r_h^*$ ,  $|\gamma| < 1.4$ , Hoekstra weight.

## E and B modes

The aperture mass dispersion (E-mode),  $\langle M_{\text{ap}}^2 \rangle$ , and the B-mode,  $\langle M_{\times}^2 \rangle$ , can be obtained by measuring the ellipticity correlation functions,

$$\xi_{\text{tt}}(\theta) = \langle \epsilon_{\text{t}} \epsilon_{\text{t}} \rangle(\theta), \quad \xi_{\times \times}(\theta) = \langle \epsilon_{\times} \epsilon_{\times} \rangle(\theta),$$

where  $\theta$  is the distance between a pair of galaxies with tangential shear  $\epsilon_{\text{ti}}$ ,  $\epsilon_{\text{tj}}$  or cross shear  $\epsilon_{\times i}$ ,  $\epsilon_{\times j}$ . With the definitions,

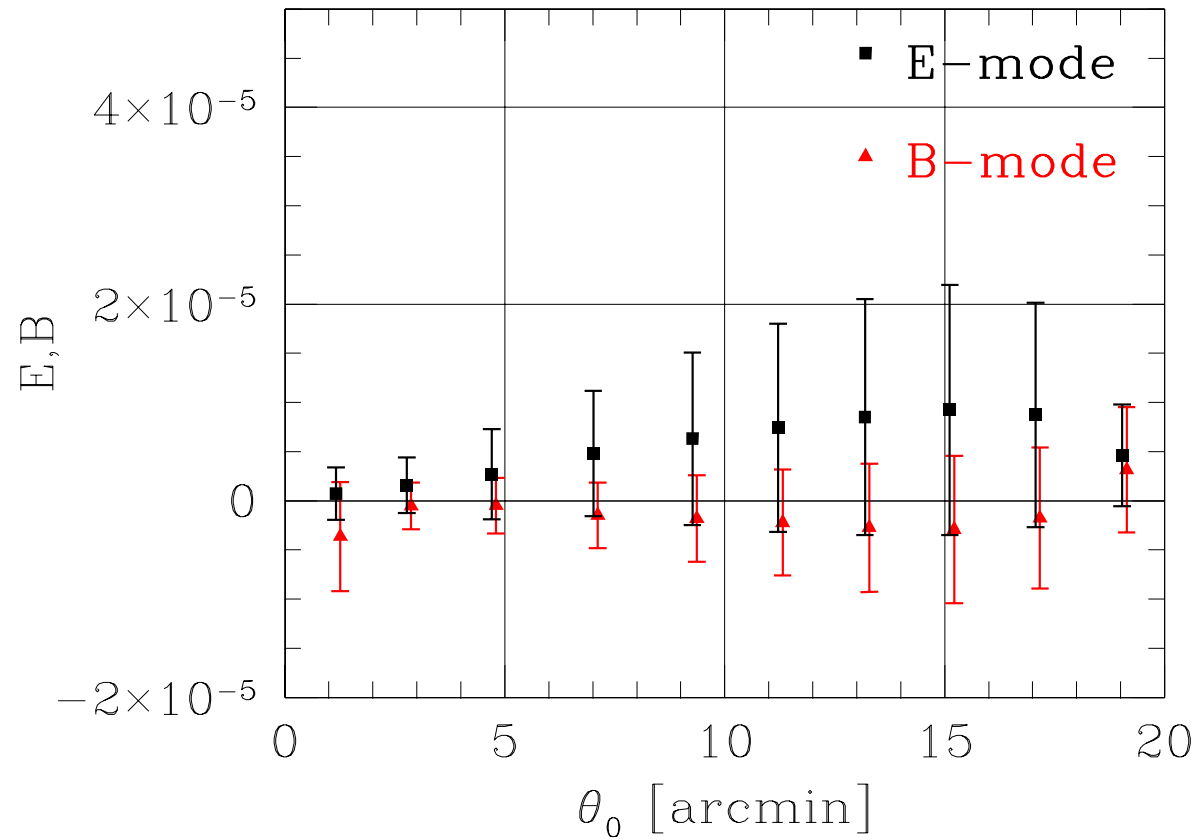
$$\xi_{\pm}(\theta) = \xi_{\text{tt}}(\theta) \pm \xi_{\times \times}(\theta),$$

it follows,

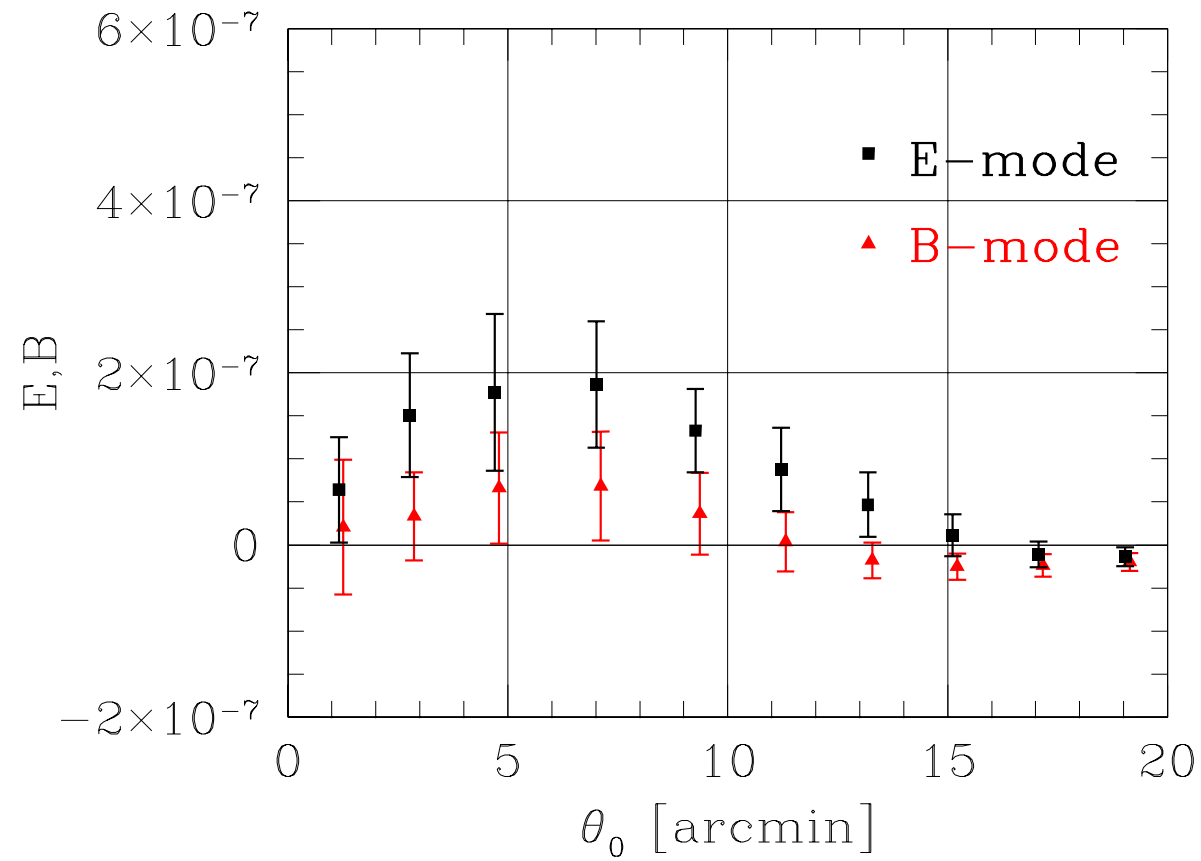
$$\langle M_{\text{ap}}^2 \rangle(\theta) = \frac{1}{2} \int d\vartheta \frac{\vartheta}{\theta_0^2} \left[ \xi_{+}(\vartheta) T_{+} \left( \frac{\vartheta}{\theta_0} \right) + \xi_{-}(\vartheta) T_{-} \left( \frac{\vartheta}{\theta_0} \right) \right].$$

$$\langle M_{\times}^2 \rangle(\theta) = \frac{1}{2} \int d\vartheta \frac{\vartheta}{\theta_0^2} \left[ \xi_{+}(\vartheta) T_{-} \left( \frac{\vartheta}{\theta_0} \right) - \xi_{-}(\vartheta) T_{-} \left( \frac{\vartheta}{\theta_0} \right) \right].$$

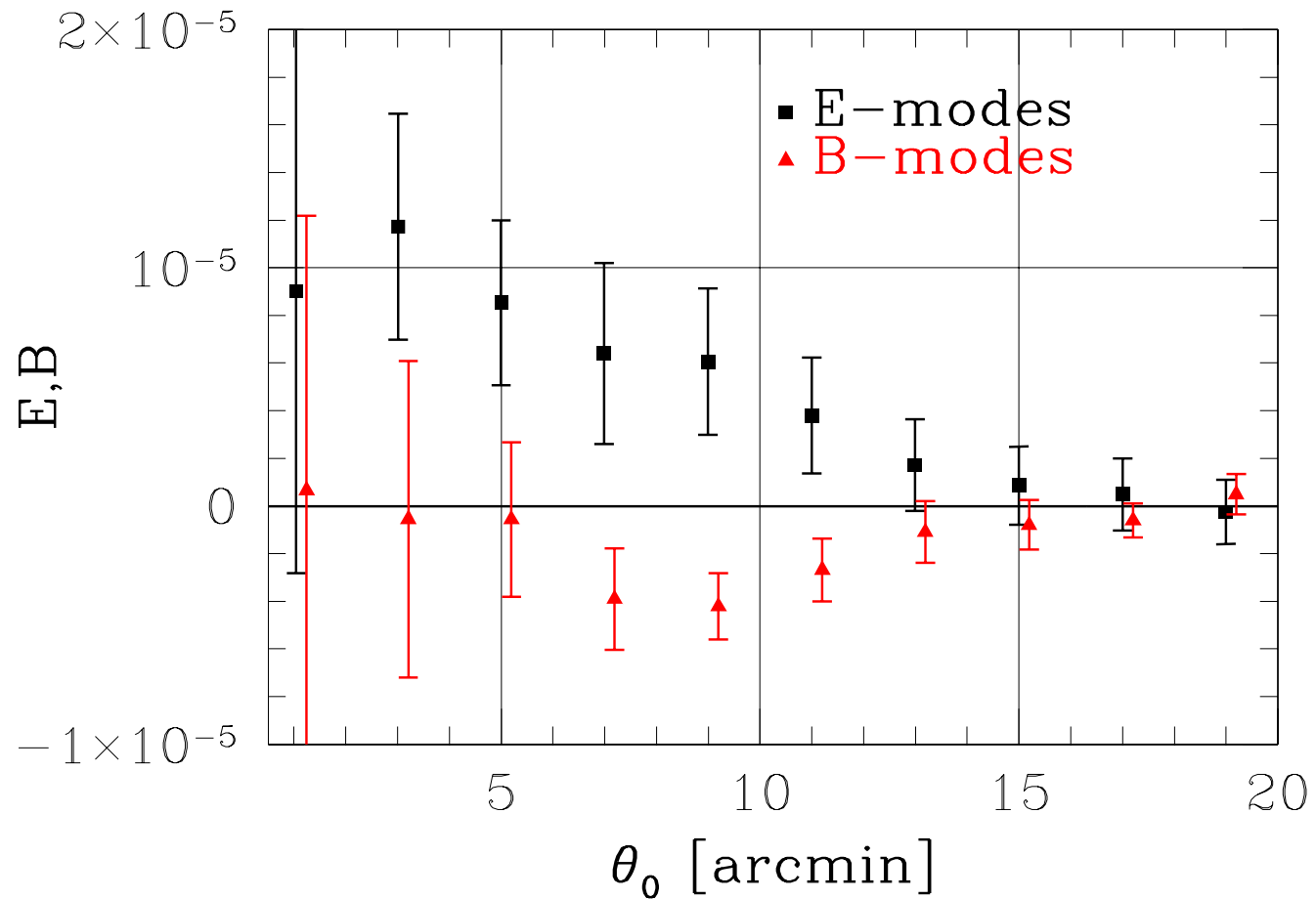
## $E$ and $B$ modes of uncorrected stars of the DPS



## $E$ and $B$ modes of anisotropy corrected stars of the DPS

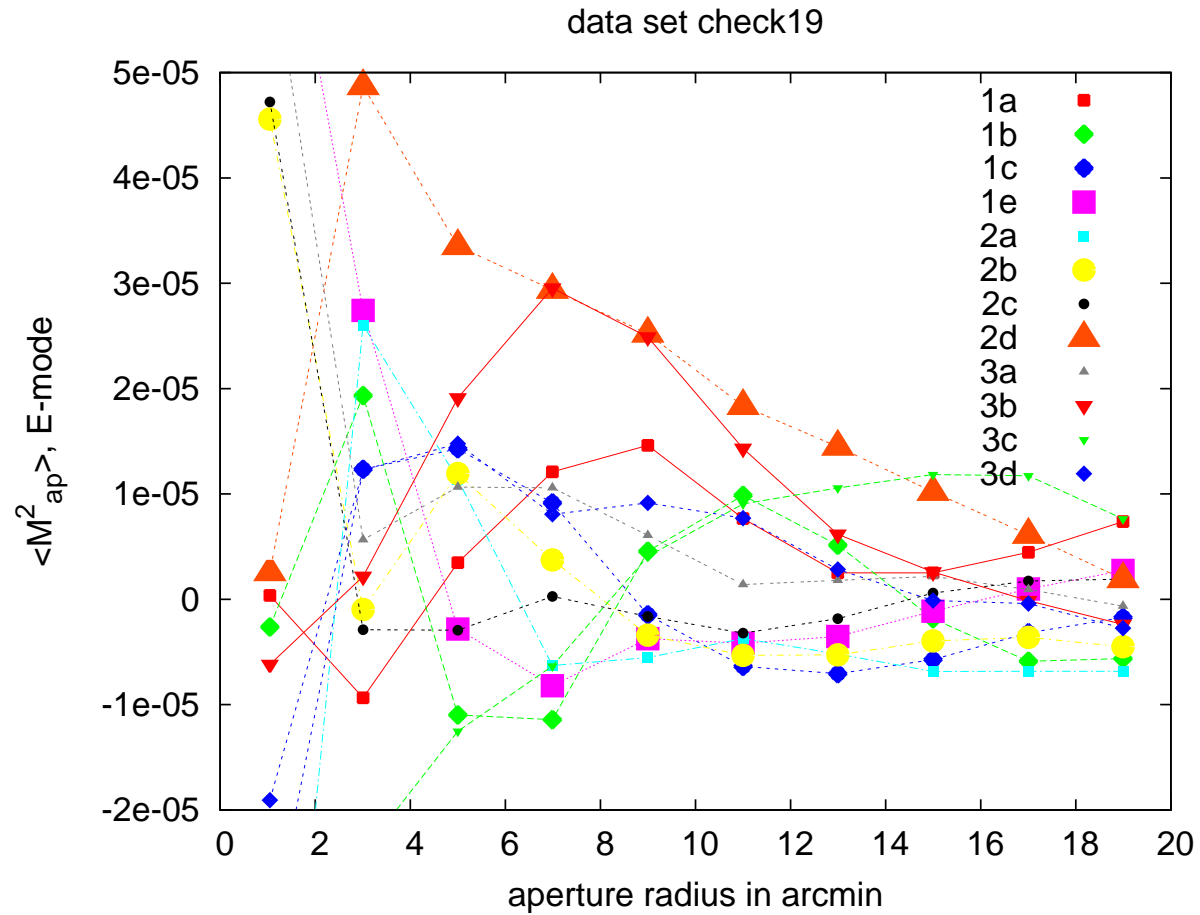


## $E$ and $B$ modes of the DPS



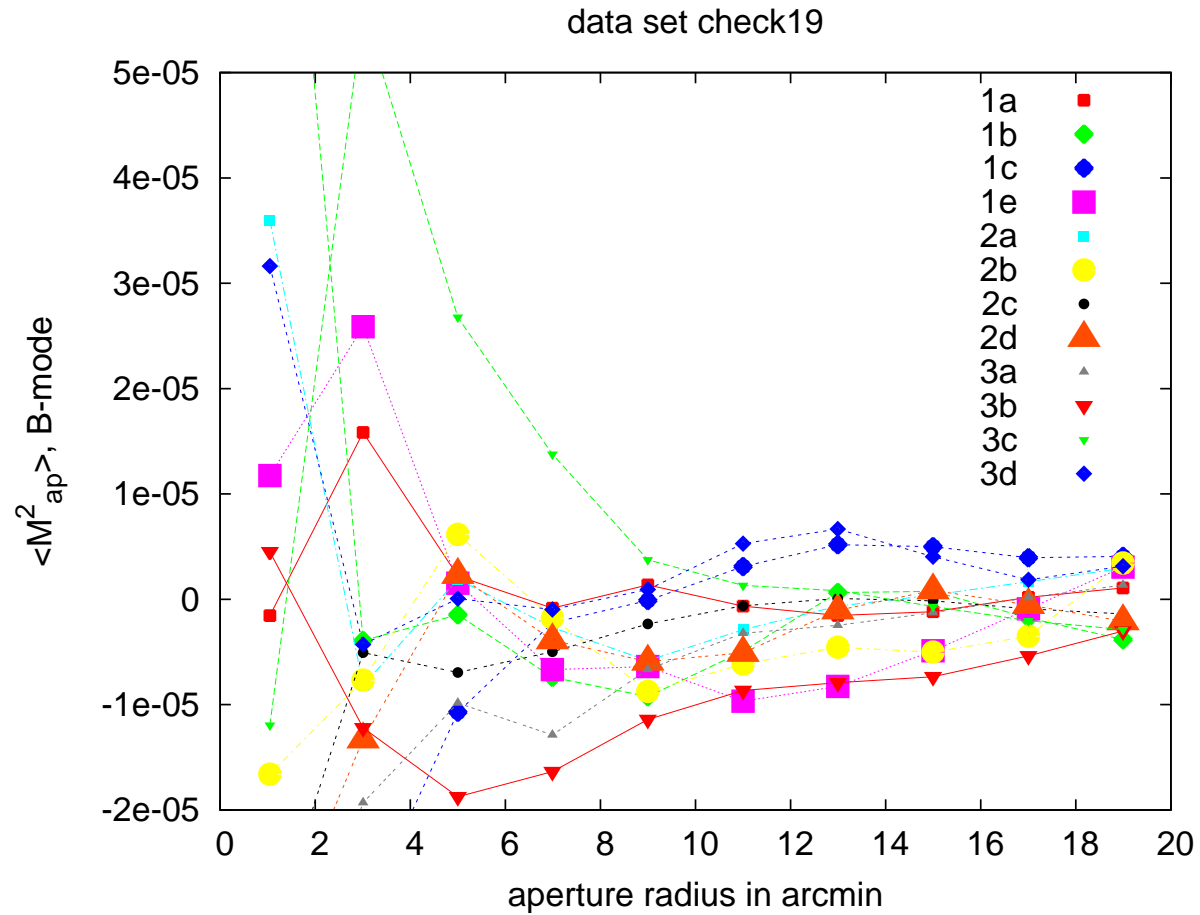
12 DPS fields,  $R$ -band,  $mag \in [21.5, 24.5]$ , no colour information yet.

## $E$ modes of all DPS fields



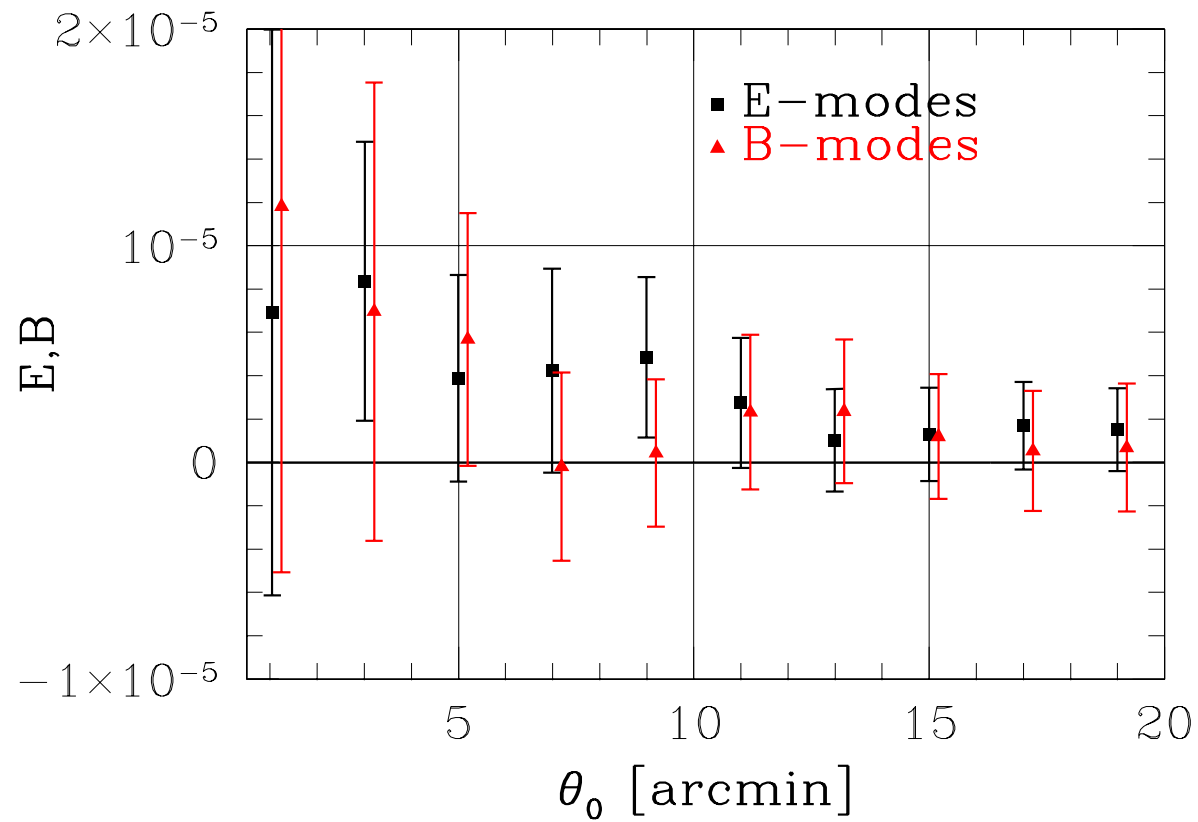
12 DPS fields,  $R$ -band,  $mag \in [21.5, 24.5]$ , no colour information yet.

## *B* modes of all DPS fields



12 DPS fields, *R*-band,  $mag \in [21.5, 24.5]$ , no colour information yet.

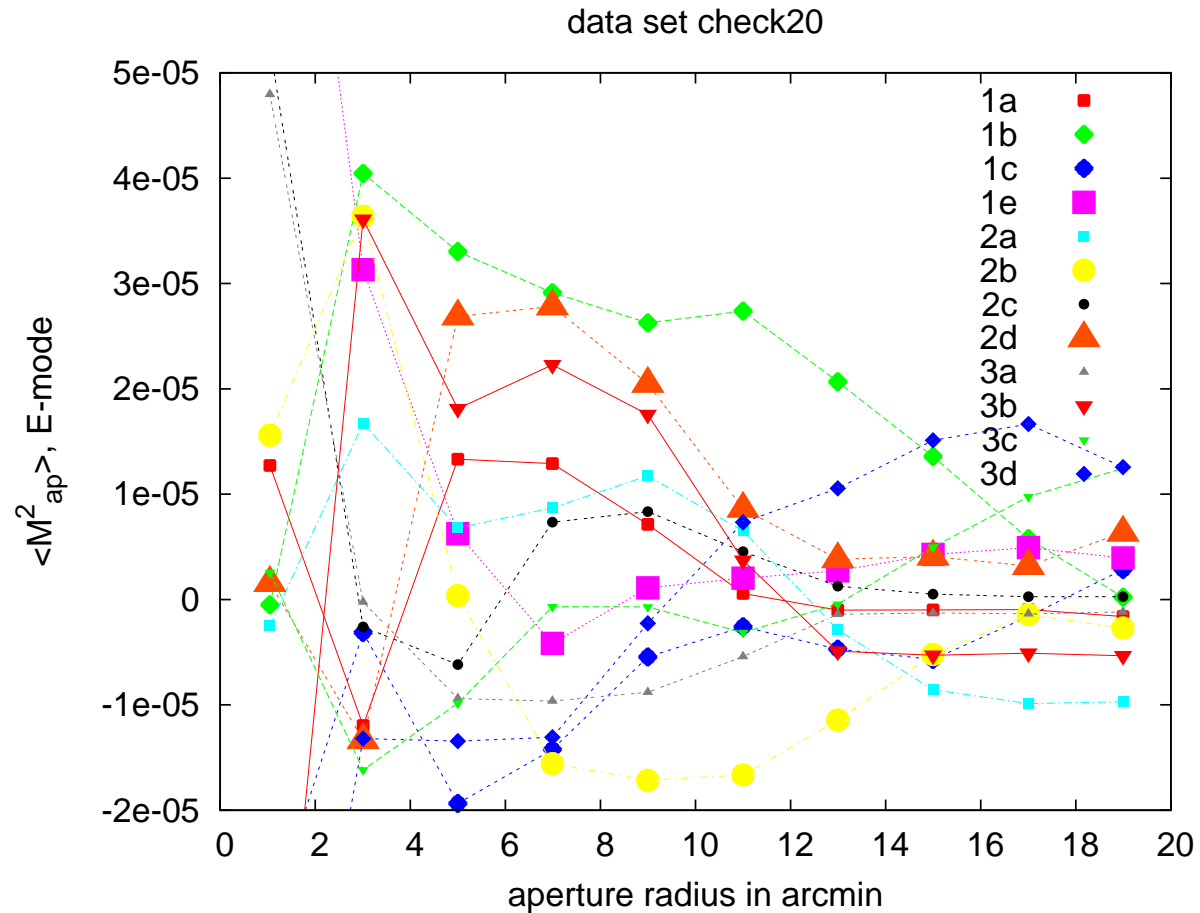
## $E$ and $B$ modes of the DPS



12 DPS fields,  $R$ -band,  $mag \in [21.5, 24.5]$ , no colour information yet,  
NOW: matrix calculation of  $P^\gamma$ .

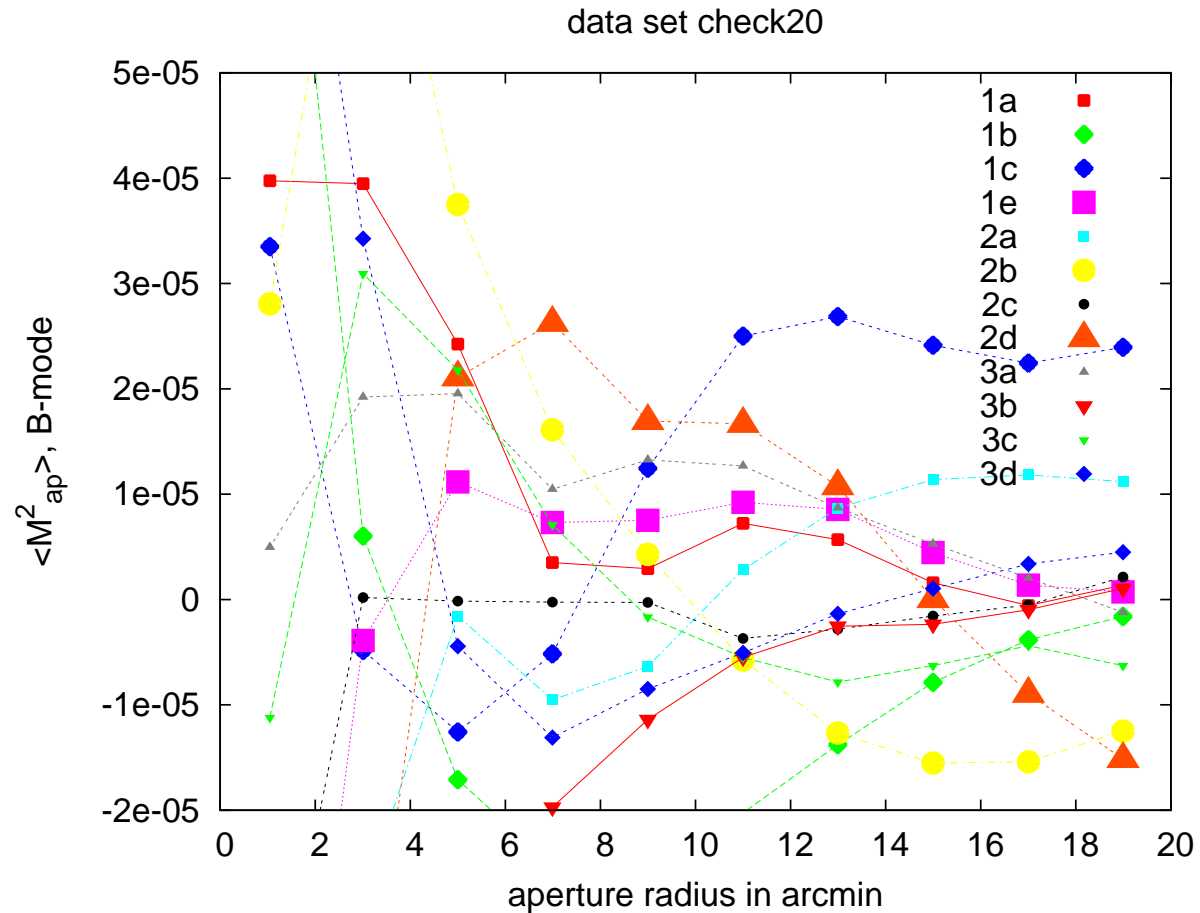


## $E$ modes of all DPS fields



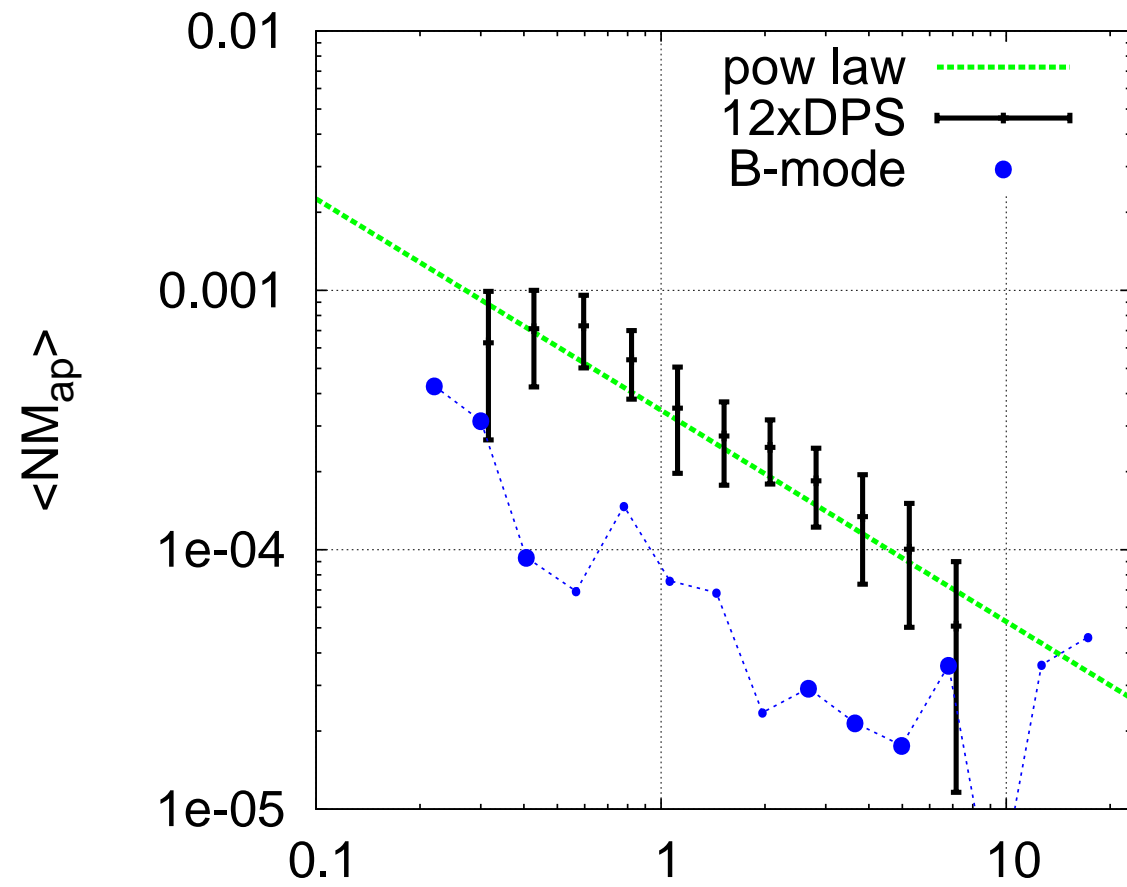
12 DPS fields,  $R$ -band,  $mag \in [21.5, 24.5]$ , no colour information yet,  
NOW: matrix calculation of  $P^\gamma$ .

## *B* modes of all DPS fields



12 DPS fields, *R*-band,  $mag \in [21.5, 24.5]$ , no colour information yet,  
NOW: matrix calculation of  $P^\gamma$ .

## $NM_{ap}$ of the DPS



## Outlook

### Improvement of $E$ , $B$ modes in the DPS:

A better anisotropy correction:

$$\chi^*(x, y) = \frac{\sum_{l,m} a_{lm} f_{lm}(x, y)}{1 + \sum_{l,m} b_{lm} f_{lm}(x, y)},$$

see Hoekstra, H. (2004) and Van Waerbeke, L. (2005).

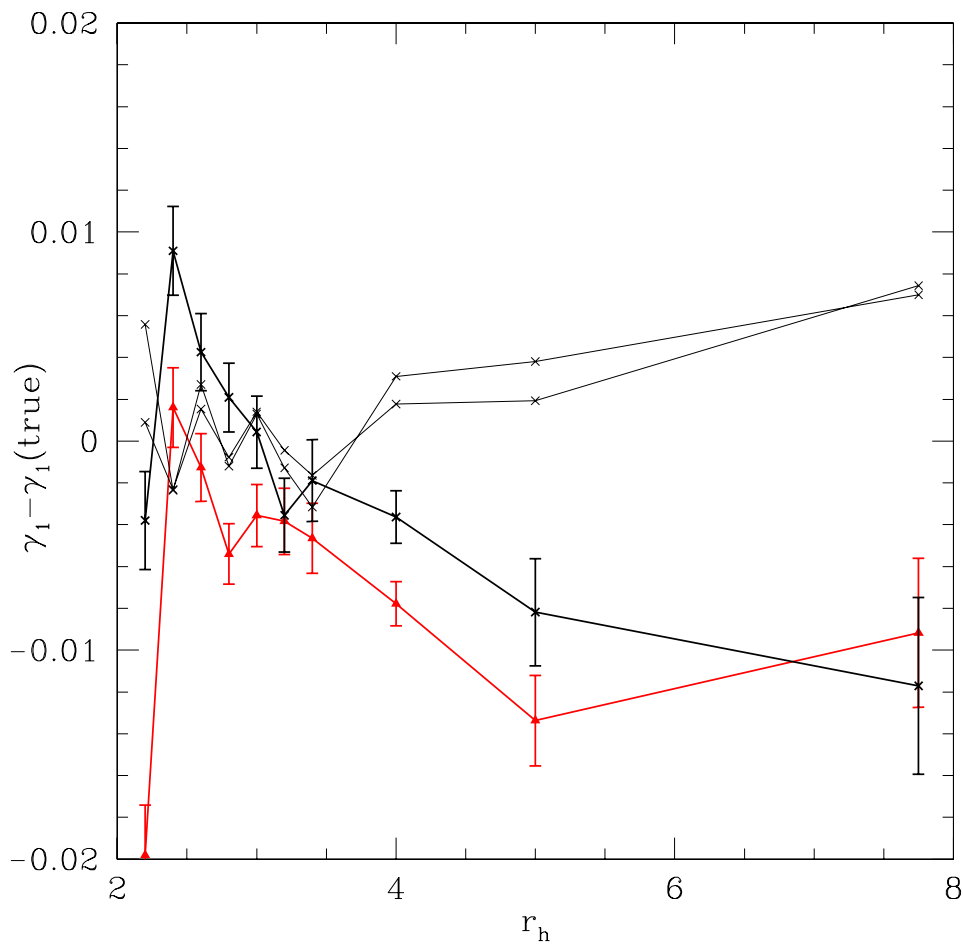
2D polynomial fit to  $P^{sh,*}/P^{sm,*}$  with a  $x$   $\sigma$ -clipping (followed by anisotropy correction without these stars).

### Improvement of simulations:

Skymaker with variable PSF (L. van Waerbeke, T. Erben),

Source clustering & shear tomography (P. Simon)

## STEP1: radius dependence of shear estimate



STEP1: psf3lens3 (defocus,  $\gamma = 0.05$ )

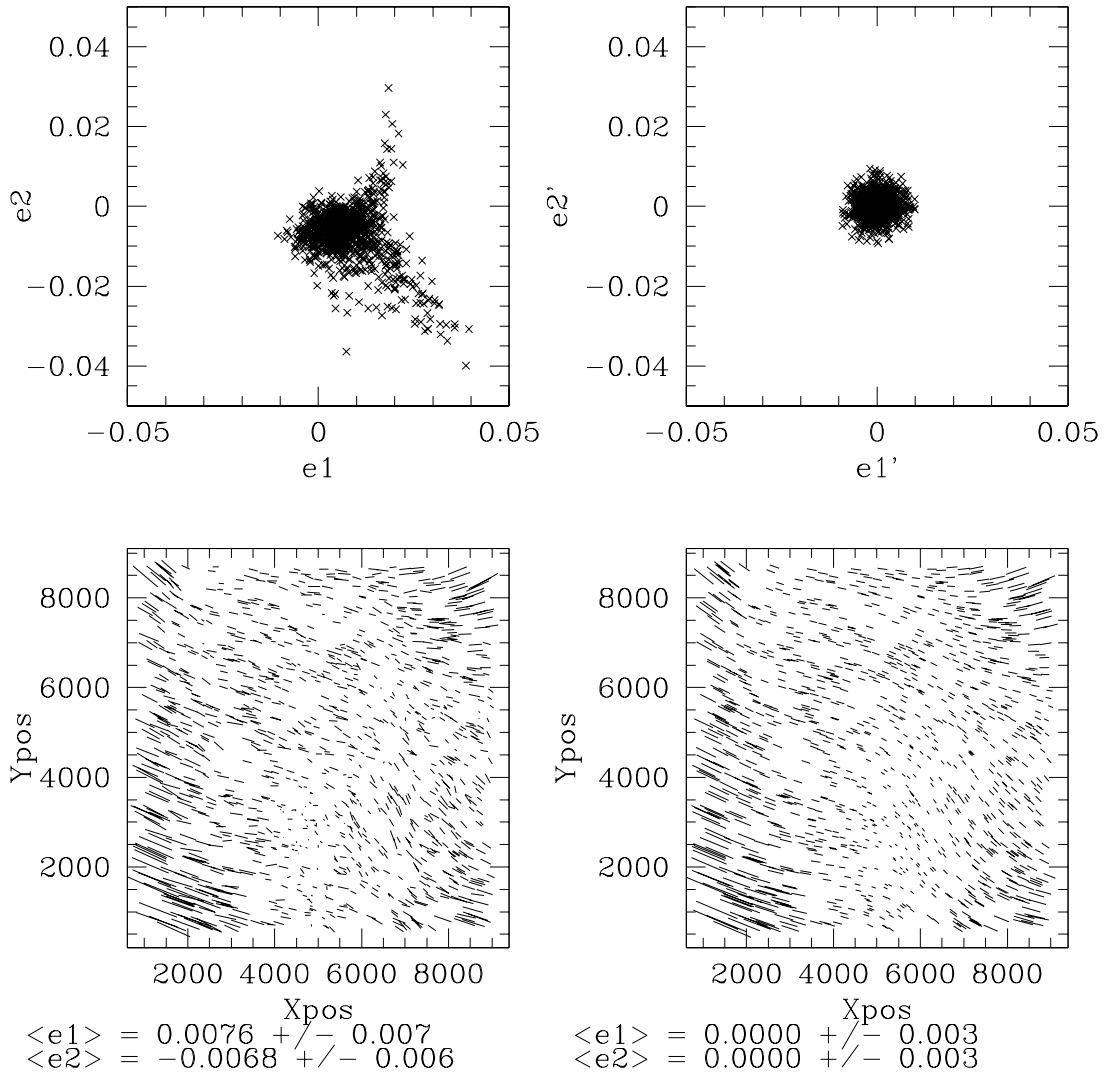
Red: former KSB implementation

solid black: NEW II (matrix calculation)

thin black: no shear

# Anisotropy correction of Deep3b

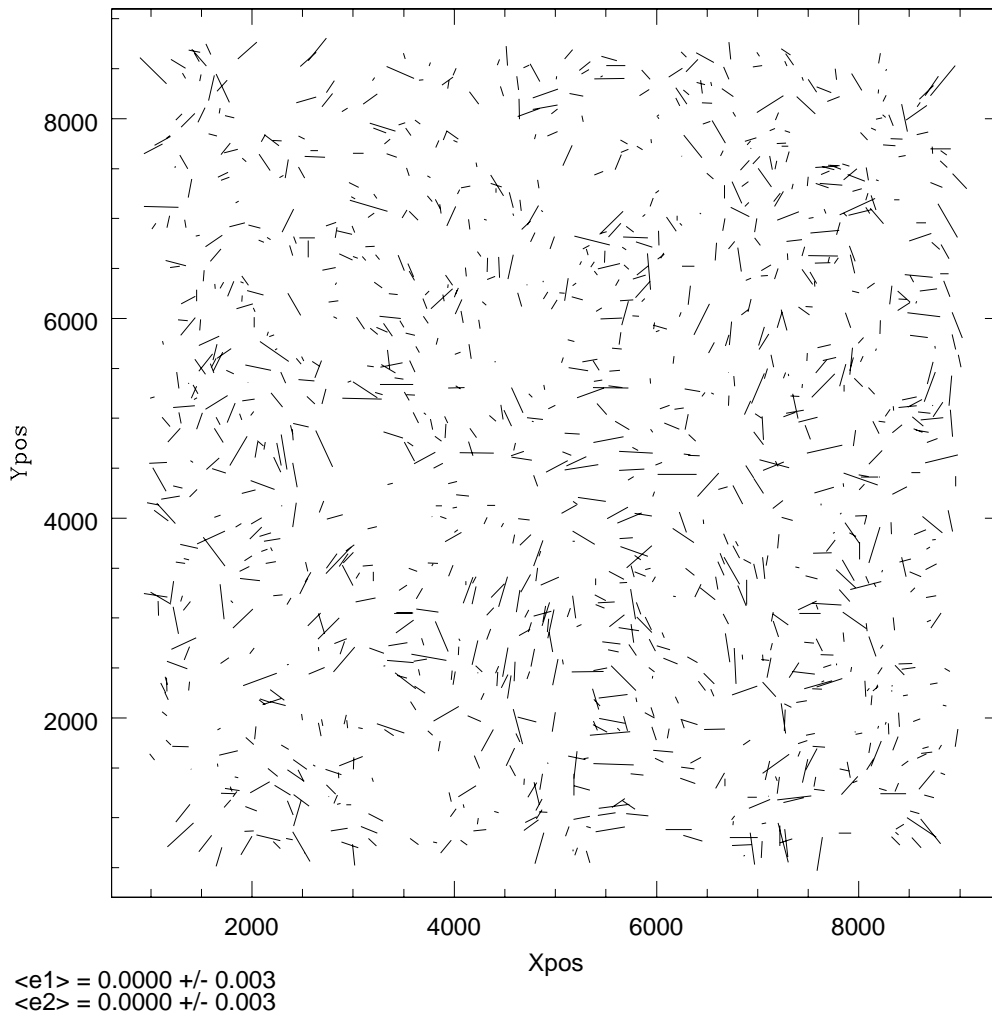
/data\_h/mhetter/DPS/R/cats/Deep3b\_r.D3BA.swarp\_anisocorr\_s.terne.cat



1179 Stars:  $x \in [1000, 9000]$ ,  $y \in [600, 8700]$ ,  $r_h \in [1.7, 2.1]$ ,  
 $mag \in [16.4, 20.6]$  and 5<sup>th</sup> order polynomial fit over the  
 whole field.

# Ellipticity pattern of stars after anisotropy correction (Deep3b)

/data<sub>h</sub>/mhetter/DPS/R/cats/Deep3b<sub>R</sub>.D3BA.swarp<sub>a</sub>nisocorr<sub>s</sub>terne.cat



1179 Stars:  $x \in [1000, 9000]$ ,  $y \in [600, 8700]$ ,  $r_h \in [1.7, 2.1]$ ,  
 $mag \in [16.4, 20.6]$  and 5<sup>th</sup> order polynomial fit over the  
whole field; largest stick  $\approx 1\%$ .